J. Fluid Mech. (2021), *vol*. 908, R3, doi:10.1017/jfm.2020.991

Reynolds number scaling of the peak turbulence intensity in wall flows

Xi Chen[1],† **and Katepalli R. Sreenivasan**[2]

[1]Key Laboratory of Fluid Mechanics of Ministry of Education, Beihang University (Beijing University of Aeronautics and Astronautics), 100191 Beijing, PR China

[2]Tandon School of Engineering, Courant Institute of Mathematical Sciences, Department of Physics, New York University, New York, NY 10012, USA

(Received 18 July 2020; revised 21 October 2020; accepted 5 November 2020)

The celebrated wall-scaling works for many statistical averages in turbulent flows near smooth walls, but the streamwise velocity fluctuation, u', is thought to be among the few exceptions. In particular, the near-wall mean-square peak, $\overline{u'u'}_p^+$ – where the superscript $+$ indicates normalization by the friction velocity u_τ, the subscript p indicates the peak value and the overbar indicates time averaging – is known to increase with increasing Reynolds number. The existing explanations suggest a logarithmic growth with respect to Re, where Re is the Reynolds number based on u_τ and the thickness of the wall flow. We show that this boundless growth calls into question the veracity of wall-scaling and so cannot be sustained, and we establish an alternative formula for the peak magnitude that approaches a finite limit $\overline{u'u'}_\infty^+$ owing to the natural constraint of boundedness on the dissipation rate at the wall. This new formula agrees well with the existing data and, in contrast to the logarithmic growth, supports the classical wall-scaling for turbulent intensity at asymptotically high Reynolds numbers.

Key words: turbulence theory, turbulent boundary layers, pipe flow boundary layer

1. Introduction

The dominant paradigm in the phenomenology of turbulent channel, pipe and boundary layers is that the flow near the wall scales solely on the kinematic viscosity ν and the wall shear stress τ_w, and that, with increasing Reynolds number, the small structure near the wall becomes increasingly independent of the large scales influenced by the flow geometry. This theme has been remarkably successful for the mean velocity, as evidenced by the law of the wall (Monkewitz, Chauhan & Nagib 2007; Nagib, Chauhan & Monkewitz 2007; Marusic *et al.* 2010; Smits, McKeon & Marusic 2011). Similar expectations for

† Email address for correspondence: chenxi97@outlook.com

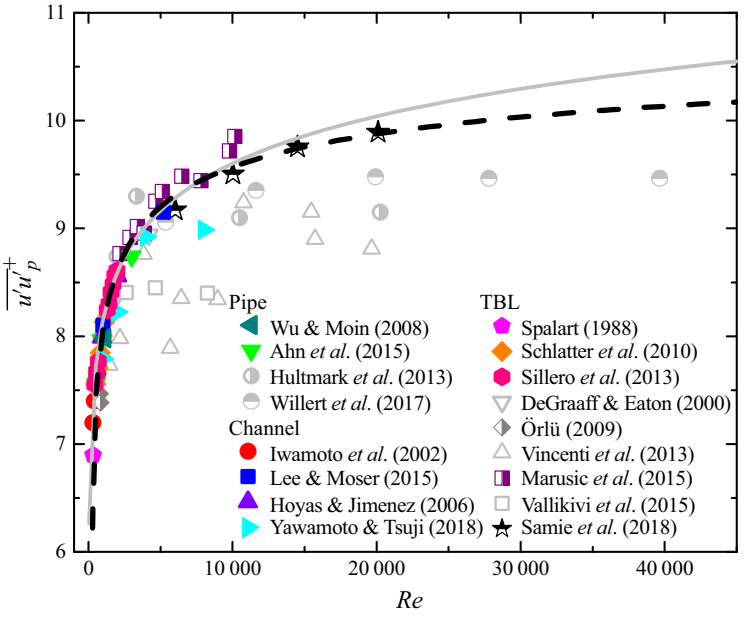

Figure 1. Reynolds number dependence of the near-wall streamwise turbulence intensity peak $\overline{u'u'}_p^+$ normalized by friction velocity square u_τ^2. Solid line indicates the logarithmic growth of (1.1) given by Marusic, Baars & Hutchins (2017); dashed line is the defect power-law growth, (4.2), newly obtained in this paper, as will be explained in the text. Symbols are for data from channel, pipe and TBL: solid symbols are from DNS and the rest from experiments. References to the data are presented in the panel.

turbulent intensities are assumed in engineering models to be independent of the Reynolds number (e.g. $k-\omega$ and $k-\epsilon$ models as reported in Wilcox 2006). Nevertheless, as found in direct numerical simulations (DNS) (Spalart 1988; Iwamoto, Suzuki & Kasagi 2002; Hoyas & Jimenez 2006; Wu & Moin 2008; Schlatter *et al.* 2009; Sillero, Jimenez & Moser 2013; Ahn *et al.* 2015; Lee & Moser 2015; Yamamoto & Tsuji 2018) as well as laboratory experiments (Sreenivasan 1989; DeGraaff & Eaton 2000; Örlü 2009; Hultmark *et al.* 2012; Vincenti *et al.* 2013; Marusic *et al.* 2015; Vallikivi, Ganapathisubramani & Smits 2015; Willert *et al.* 2017; Samie *et al.* 2018), the streamwise turbulence intensity, the dominant contributor to turbulent fluctuations, exhibits a notable dependence on the Reynolds number. As summarized in figure 1, the normalized peak value, $\overline{u'u'}_p^+$, exhibits an almost 150 % growth for Re of the order 10^2 to 10^4; here, Re is the Reynolds number based on $u_\tau = {\tau_w}^{1/2}$ and the flow thickness is δ; here and elsewhere, superscript $+$ indicates the normalization by wall variables u_τ and ν, and the overbar indicates the time average. This feature cannot be explained away by stating that the flow has not reached a fully developed state, and so triggers a challenge for the classical wall-scaling for turbulent intensity, particularly for high-Re predictions.

For the last two decades, considerable effort has been devoted to understanding this growth, almost all of which (see Marusic, Baars & Hutchins (2017) and references therein) proposes the logarithmic form

$$\overline{u'u'}_p^+ = A \ln Re + B, \tag{1.1}$$

where A and B are constants. The reason for this logarithmic growth, according to Marusic *et al.* (2017), is the inner–outer interaction between near wall and outer flow eddies,

captured in good measure by the attached-eddy model of Townsend. The inner–outer interaction can also be understood from the perspective of mixed scaling (Sreenivasan 1989; DeGraaff & Eaton 2000), according to which turbulence intensity scales as the geometric mean of u_τ and $\bar{u}_e$, where $\bar{u}_e$ is the centreline velocity of channel and pipe, or the free-stream velocity of the turbulent boundary layer (TBL). We thus have

$$\overline{u'u'}_p^+ \equiv \frac{\overline{u'u'}_p}{u_\tau^2} = \frac{\overline{u'u'}_p}{u_\tau \bar{u}_e}\frac{\bar{u}_e}{u_\tau} \propto \frac{\bar{u}_e}{u_\tau} \propto \ln Re, \tag{1.2}$$

where, in the last step, we have used the well-known result from the log-law for the mean velocity $\bar{u}$, which gives $\bar{u}_e/u_\tau \propto \ln Re$. With the two fitting parameters $A = 0.63$ and $B = 3.80$ given in Marusic *et al.* (2017), (1.1) represents the data quite well, as the solid line in figure 1 shows. If it continues to remain valid for very high Re, the logarithmic growth indicates the failure of the wall-scaling for turbulence intensity. The dashed line is the alternative result derived here. The rest of the paper is concerned with its derivation and interpretation.

Before proceeding further, we should note that Monkewitz & Nagib (2015) have questioned the mixed scaling for $\overline{u'u'}$ in TBL. They found that the mixed scaling is ruled out for the logarithmic mean velocity profile if one assumes that the Reynolds normal stress term $\partial_x\overline{u'u'}$ is of the same order as the mean convective terms $\bar{u}\partial_x\bar{u} + \bar{v}\partial_y\bar{u}$ (where v is the wall-normal velocity). This argument leads to the classical viscous scaling for near-wall $\overline{u'u'}$ and implies a finite near-wall peak as $Re \to \infty$. By examining the available data, these authors further suggested that the asymptotic peak value is approximately 22 and the departure from this asymptote has the form $1/\ln(Re)$, i.e. $\overline{u'u'}_p^+ \approx 22\text{–}340/\bar{u}_e^+$. However, their analysis does not necessarily exclude mixed scaling if $\partial_x\overline{u'u'}$ scales differently (e.g. as the residue between the derivatives of viscous shear and Reynolds shear stress) – without causing a problem for the momentum balance. Moreover, as noted by Monkewitz & Nagib (2015), their analysis is restricted to TBL but not applicable to channel and pipe flows, as the latter two have no $\partial_x\overline{u'u'}$ term in the mean momentum equation. Yet, all three flows show a similar Re-dependence of $\overline{u'u'}_p^+$. Therefore, mere order of magnitude analysis cannot provide a conclusive answer for the scaling of $\overline{u'u'}$, and a common explanation on the Re-dependence of peak value for the three flows is still desired.

2. A plausible argument against the continued growth of $\overline{u'u'}_p^+$

We now demonstrate that any sustained growth of $\overline{u'u'}_p^+$, such as the logarithmic growth of (1.2), comes with a difficulty. The balance equation of $\overline{u'u'}$, derived from Navier–Stokes equations, presented here in a general form for the channel, pipe and TBL, reads as

$$S^+W^+ + \mathcal{D}^+ - \epsilon^+ = \mathcal{N}^+, \tag{2.1}$$

where the turbulent production $\mathcal{P}^+ = S^+W^+$ is the product of the mean shear $S^+ = \partial\bar{u}^+/\partial y^+$ and Reynolds shear stress $W^+ = -\overline{u'v'}^+$, turbulent diffusion is given by $\mathcal{D}^+ = \frac{1}{2}(\partial^2/\partial y^{+2})\overline{u'^2}^+$, the dissipation by $\epsilon^+ = \overline{|\nabla u'|^+}^2$ and $\mathcal{N}^+$ includes the transport term and nonlinear correlation of pressure and velocity fluctuations. Very close to the wall, the leading order balance in (2.1) is between diffusion and dissipation (Chen, Hussain &

She 2018), this being exact at the wall so that

$$\mathcal{D}_w^+ = \epsilon_w^+, \tag{2.2}$$

with the subscript w indicating conditions at the wall. By the Taylor expansion of $\overline{u'u'}^+$, i.e. $\overline{u'u'}^+ = \mathcal{D}_w^+ y^{+2}$+ high order terms, one can estimate the order of the peak value located at y_p^+ as

$$\overline{u'u'}_p^+ \sim \mathcal{D}_w^+ y_p^{+2} = \epsilon_w^+ y_p^{+2} \tag{2.3}$$

(where the '$\sim$' sign represents an estimate from the expansion and the '$=$' sign results from (2.2)). To understand the behaviour of this equation as $Re \to \infty$, note that all available evidence (see e.g. Sreenivasan 1989; Metzger & Klewicki 2001; Lee & Moser 2015) suggests that the position y_p^+ of $\overline{u'u'}_p^+$ is remarkably independent of the Reynolds number. Thus, (2.3) should be a reasonable order of magnitude estimate in the large-Re limit. If so, any boundless increase of the left-hand side of (2.3) with respect to Re would mean that $\epsilon_w^+ \to \infty$, which is an implausible result.

The most important reason for expecting ϵ_w^+ to be bounded is as follows. The energy production essentially balances dissipation in the region of peak production. Therefore, an infinite dissipation would imply an infinite production but it is well known (Sreenivasan 1989; Chen *et al*. 2018) that, in these units, the maximum production is bounded by 1/4. To see this, note that the mean momentum balance near the wall approximates to

$$S^+ + W^+ \approx 1, \tag{2.4}$$

which yields the maximum for S^+W^+ when $S^+ = W^+ = 1/2$ (around $y^+ \approx 12$ as summarized, e.g. in Sreenivasan (1989), She, Chen & Hussain (2017) and Cantwell (2019). That is,

$$\mathcal{P}_\infty^+ = (S^+W^+)_{max} = (1/2) * (1/2) = 1/4. \tag{2.5}$$

This bound on the production argues against a boundless increase of the wall dissipation even in the limit of infinite Reynolds number. We are thus driven to find an alternative scaling rather than persist with the logarithmic growth of the peak in the streamwise velocity fluctuation.

3. Scaling of the dissipation rate at the wall

If every term in (2.1) is surmised to be bounded, we define the amount of dissipation rate that departs from its limiting value $\epsilon_\infty^+ = 1/4$ as

$$\epsilon_d^+ = \epsilon_\infty^+ - \epsilon_w^+ = 1/4 - \epsilon_w^+. \tag{3.1}$$

The quantity $\epsilon_d^+ = \epsilon_d/(u_\tau^4/\nu)$, which is the 'defect' dissipation that falls short of the asymptotic maximum of 1/4, is relevant to our analysis of how the dissipation near the wall asymptotes to the limit. A similar defect quantity, defined for the maximum Reynolds shear stress in Chen, Hussain & She (2019), reveals a non-universal scaling transition of momentum transfer among channel, pipe and TBL flows.

If the energy dissipation near the wall were to follow the wall-law, as might be expected for infinitely large Reynolds number, it would be given by $u_\tau^2/(\nu/u_\tau^2) = u_\tau^4/\nu$. (One can also obtain this result, as did Monkewitz & Nagib (2015), by integrating the suitably normalized form of Kolmogorov's $-5/3$ spectrum for $\overline{u'u'}$.) At any finite Reynolds number, however, the energy dissipation near the wall falls short of u_τ^4/ν because some

of the energy produced there is transmitted to the outer layer without getting dissipated locally, and this happens presumably over a typical time scale that is smaller than δ/u_τ but larger than ν/u_τ^2, as suggested by past studies of turbulent bursting (Rao, Narasimha & Narayanan 1971). One might regard this time scale as the one that the outer layer imposes on the inner layer – small for the outer layer but large for the inner layer. A conjecture is that this scale is given by η_o/u_τ, where u_τ is the typical velocity scale for wall flows while the length scale η_o is the key assumption, proposed as the smallest (Kolomogorov) length for the outer region given by

$$\eta_o = \nu^{3/4}/\epsilon_o^{1/4}; \quad \epsilon_o = u_\tau^3/\delta, \tag{3.2a,b}$$

where the subscript 'o' refers to the outer region of the wall flow (ϵ_o is the outer dissipation scale). Accordingly, we have

$$\epsilon_d \sim u_\tau^3/\eta_o \sim \varepsilon_o Re^{3/4}, \tag{3.3}$$

where we used (3.2*a*,*b*) (in this section, the sign '$\sim$' means 'scales as'). Putting (3.3) in wall units, we get

$$\epsilon_d^+ = \epsilon_d/(u_\tau^4/\nu) \sim \epsilon_o Re^{3/4}/(u_\tau^4/\nu) \sim Re^{-1/4}, \tag{3.4}$$

from which it follows that

$$\epsilon_w^+ = 1/4 - \epsilon_d^+ = 1/4 - \beta/Re^{1/4}. \tag{3.5}$$

Clearly ϵ_d^+ decreases with increasing Re, and (3.5) shows how ϵ_w^+ approaches its upper limit of a 1/4. In figure 2(*a*), we display the defect dissipation rate versus Re and observe an excellent $-1/4$ power, as given by (3.5). The only fitting parameter is the proportionality coefficient $\beta \approx 0.42$, estimated from the DNS data at $Re = 1000$, which is the middle of the range covered here. Note that the time scale η_o/u_τ is proposed to be the same for channel, pipe and TBL flows, while the proportionality coefficient β – attributed to the outer flow influence – may be flow dependent. The geometry effect on the near-wall quantities, as well as uncertainty on the wall-dissipation data (through direct and indirect estimation), are important and deserve a thorough investigation in the future, and are not discussed here. Moreover, figure 2(*b*) compares (3.5) with the logarithmic fit by Tardu (2017), i.e. $\epsilon_w^+ = 0.02 \ln Re + 0.035$, and shows that the present fit describes the data better.

It should be stressed that (3.3) contains specific physics which can be tested more directly than is done here. Essentially, the physics is that the smallest scale in the outer layer, given by its characteristic Kolmogorov scale, is the largest scale that the wall layer sees. Thus, the effective range of scales available to the energetics of the wall layer ranges between η_0 and local η, with their ratio given by $Re^{1/4}$.

4. Scaling of streamwise turbulence intensity peak

Substituting (3.5) into (2.3) yields

$$\overline{u'u'}_p^+ \sim \mathcal{D}_w^+ y_p^{+2} = \epsilon_w^+ y_p^{+2} = (1/4 - \beta\, Re^{-1/4}) y_p^{+2}, \tag{4.1}$$

which can be rewritten as

$$\overline{u'u'}_p^+ = \alpha(1/4 - \beta\, Re^{-1/4}) = \overline{u'u'}_\infty^+ - \gamma\, Re^{-1/4}, \tag{4.2}$$

where $\overline{u'u'}_\infty^+ = \alpha/4$ (α is a proportional coefficient) and $\gamma = \alpha\beta$. At the typical Reynolds number of 1000, $\overline{u'u'}_p^+ \approx 8.1$ from DNS data (Lee & Moser 2015); taken together with

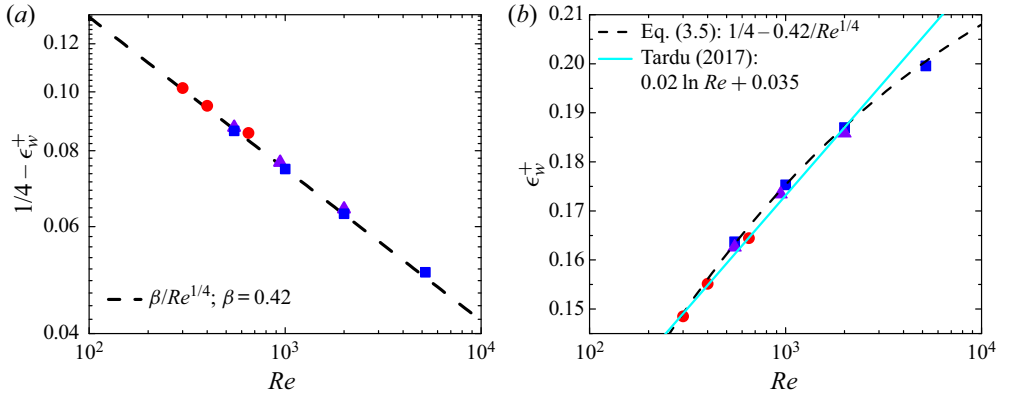

Figure 2. (*a*) The defect dissipation rate at the wall from its upper bound of 1/4 showing an excellent $Re^{-1/4}$ fit as predicted by (3.5), dashed line. (*b*) Wall-dissipation rate varying with Re in close agreement with (3.5), dashed line; also included for comparison is the logarithmic fitting by Tardu (2017), i.e. $0.02 \ln Re + 0.035$, solid line. Symbols are from DNS data in channel flows at different values of Re. For the data legend, see figure 1.

$\beta \approx 0.42$ shown in figure 2, we get $\alpha \approx 46$ from (4.2). (It will be shown by a different reasoning in § 5 that α is close to $y_p^{+2}/4 \approx 49$.) We also have $\gamma \approx 19.32$ and $\overline{u'u'}^+_\infty = \alpha/4 \approx 11.5$, this being our predicted asymptotic peak value as $Re \to \infty$.

Validations of (4.2) with $\alpha = 46$ and $\beta = 0.42$ are shown in figures 1 and 3. For comparison, we have collected data of three wall flows from both DNS and experimental measurements. Not only are the DNS data with the highest Re reported in literature included – Re up to 8000 for channel (Yamamoto & Tsuji 2018), 3000 for pipe (Ahn *et al.* 2015) and 2000 for TBL (Sillero *et al.* 2013) – but also included are other DNS data of channels (Iwamoto *et al.* 2002; Hoyas & Jimenez 2006; Lee & Moser 2015), pipes (Wu & Moin 2008) and TBL (Spalart 1988; Schlatter *et al.* 2009). Experimental data for pipes and TBL from worldwide facilities (DeGraaff & Eaton 2000; Örlü 2009; Hultmark *et al.* 2012; Vincenti *et al.* 2013; Marusic *et al.* 2015; Vallikivi *et al.* 2015; Willert *et al.* 2017; Samie *et al.* 2018) are collected as well. These data cover more than two decades in Re, offering a good benchmark for validating the proposed scaling law. Note that differing from Marusic *et al.* (2017) where Re of TBL was defined by the thickness obtained via mean velocity log-law fitting (see Marusic *et al.* (2015) for details), we use δ_{99} as the boundary layer thickness and hence $Re = u_\tau \delta_{99}/\nu$ for TBL flows. Also, data of Vincenti *et al.* (2013) are not taken from any plot in Marusic *et al.* (2017) but from original data authors.

As shown in figure 1, (4.2) agrees closely with data. Experimental data show considerable scatter, which is not surprising because the accurate measurement of $\overline{u'u'}$ is still a challenging task due to limited resolution in experimental techniques (see discussions in Örlü & Alfredsson 2013; Samie *et al.* 2018). The lack of resolution is more grievous at larger Re, which may cause the apparent saturation judged from the largest Re measurements in Hultmark *et al.* (2012), Willert *et al.* (2017) and Vallikivi *et al.* (2015), represented by the grey symbols in figure 1. Except for these data, all the others display a clear monotonic increase with Re, well captured by (4.2). Further, the very recent measurements by Princeton group (Smits 2019) have started to exhibit a Re-dependent increase of the near-wall peak.

A few further comments are useful. Figure 3 shows that the data depart from (1.1) towards small Re. Considering the fact that parameters $A = 0.63$ and $B = 3.80$ in Marusic

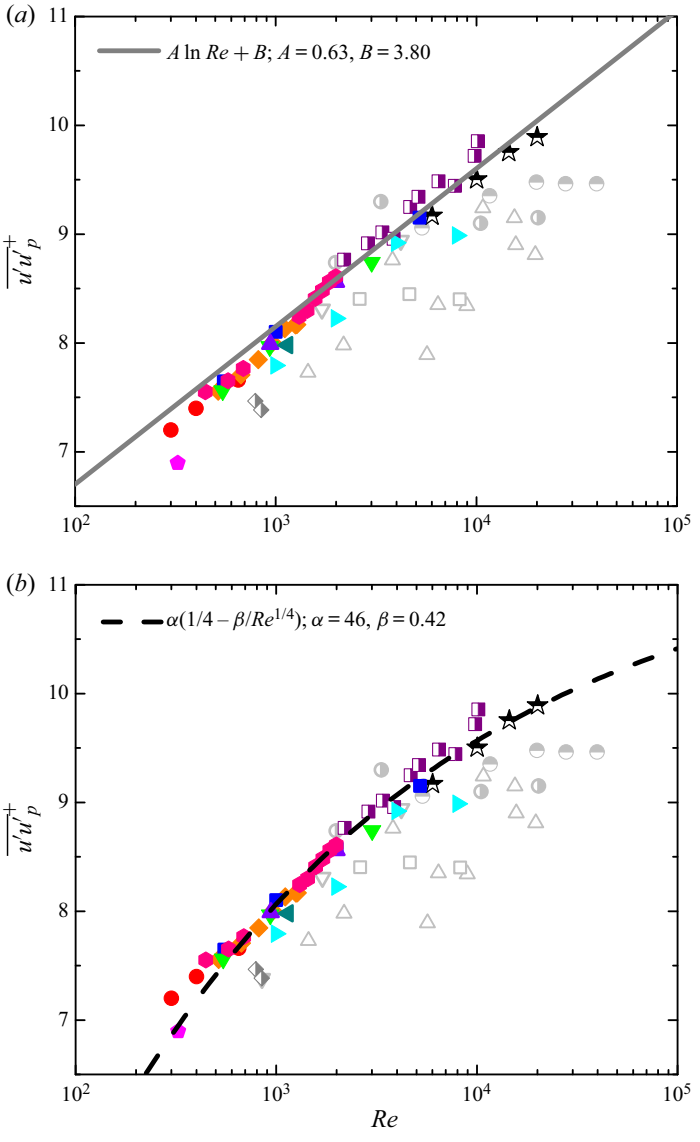

Figure 3. Streamwise turbulence intensity peak versus the logarithm of Re. Panel (*a*) compares data with (1.1) given by Marusic, Baars & Hutchins (2017), solid line; Panel (*b*) compares the same data with (4.2), dashed line. Data are the same as in figure 1.

et al. (2017) are chosen for the best fit of high-Re data, they can indeed be readjusted to reduce the departure at small Re but this would ruin the agreement with higher Re. What is clear is that the data from $Re = 500$ to 2000 exhibit a steeper slope (i.e. $A \approx 0.75$) than data from $Re = 2000$ to 20 000 (with $A \approx 0.63$), and an overall concave trend might be inferred. This feature is depicted well by (4.2), which agrees with the data. It is of interest to note that, in the atmospheric surface layer measured over the salt flats of the Great Salt Lake Desert, Metzger & Klewicki (2001) observed that $\overline{u'u'}_p^+$ occurs around 13.4 at $Re = 9 \times 10^5$, with the uncertainty between 11.6 and 15.2. The lower bound is consistent with our estimation of 11.5 from (4.2). Therefore, we might reasonably surmise that the

formula (4.2) presents a universal scaling law for the three flows of channel, pipe and TBL, with the advantage of a finite limiting value as *Re* increases.

5. Discussion

An issue to clarify is why (4.2) works well for the peak magnitude without demanding anything specifically about the non-monotonicity of $\overline{u'u'}^+$. A superficial view is that the deviation of the inner $\overline{u'u'}^+$ profile from the expansion (2.3) or (4.1) is not large at the peak location y_p^+. The underlying reason is that the higher-order terms beyond the Taylor expansion are now accounted for by the proportional coefficient $\alpha/y_p^{+2} \approx 0.23$ – close to $1/4$ – in (4.2). To see this, we develop the following analysis.

First, due to the no-slip wall condition, Reynolds shear stress has the expansion

$$-\overline{u'v'} \propto y^3, \quad or \quad -\overline{u'v'}^+ \approx Cy^{+3}, \tag{5.1a,b}$$

where C is a proportionality coefficient. In Chen *et al*. (2018), a higher-order expression of $\overline{u'v'}^+$ was obtained by introducing the length function $\ell = \sqrt{-\overline{u'v'}^+}/(\mathrm{d}\bar{u}^+/\mathrm{d}y^+)$. Accordingly, the momentum equation (2.4) can be written as

$$-\overline{u'v'}^+ + \sqrt{-\overline{u'v'}^+}/\ell^+ \approx 1. \tag{5.2}$$

Considering only the leading order balance of (5.2), i.e. $\sqrt{-\overline{u'v'}^+}/\ell^+ \approx 1$, one has

$$\ell^+ \approx C^{1/2} y^{+3/2}. \tag{5.3}$$

On the other hand, with all terms in (2.4) included, (5.2) leads to the analytical expression

$$-\overline{u'v'}^+ = 1 - \frac{2}{1+\sqrt{1+4\ell^{+2}}}. \tag{5.4}$$

Interestingly, the substitution of (5.3) in (5.4) yields

$$-\overline{u'v'}^+ \approx 1 - \frac{2}{1+\sqrt{1+4Cy^{+3}}}. \tag{5.5}$$

If $\overline{u'u'}^+ \sim \mathcal{D}_w^+ y^{+2} = \epsilon_w^+ y^{+2}$, one gets that $-\overline{u'u'}^+/\overline{u'v'}^+ \approx C'/y^+$ with $C' \approx \epsilon_w^+/C$, and from (5.5) we have

$$\overline{u'u'}^+ \approx \frac{C'}{y^+}\left[1 - \frac{2}{1+\sqrt{1+4Cy^{+3}}}\right]. \tag{5.6}$$

As verified in Chen *et al*. (2018), the above approximation depicts a non-monotonic variation of $\overline{u'u'}$ and agrees well with data from the wall up to $y^+ \approx 30$, well beyond the near-wall peak. Hence, it is reasonable to use (5.6) to estimate the peak of $\overline{u'u'}^+$ by

setting $\mathrm{d}\overline{u'u'}^{+}/\mathrm{d}y^{+} = 0$. Equation (5.6) then leads to

$$y_p^+ \approx 2^{1/3} C^{-1/3}; \tag{5.7}$$

substituting (5.7) into (5.6) one obtains the peak magnitude to be

$$\overline{u'u'}_p^{+} \approx 2^{-4/3} C^{-2/3} \epsilon_w^+ \approx (y_p^{+2}/4)\epsilon_w^+. \tag{5.8}$$

Comparing (5.8) with (4.2), we obtain the estimates

$$\alpha \approx y_p^{+2}/4; \quad \overline{u'u'}_\infty^{+} = \alpha/4 \approx y_p^{+2}/16. \tag{5.9a,b}$$

This result explains that in (4.1) and (4.2), the anticipated higher-order corrections to the Taylor expansion are now accounted for by the proportional coefficient $\alpha/y_p^{+2} \approx 1/4$. The new physics involved here are the Reynolds shear stress in (5.5) and the invariance of the ratio between $\overline{u'u'}^{+}$ and $\overline{u'v'}^{+}$ – both verified in Chen *et al.* (2018). With $y_p^+ = 14$, we have $\alpha \approx 49$ from (5.9*a*,*b*), and hence $\overline{u'u'}_\infty^{+} \approx 12.2$, very close to $\alpha \approx 46$ and $\overline{u'u'}_\infty^{+} = \alpha/4 \approx 11.5$ used for data comparisons in figures 1 and 3. The estimates again demonstrate that the peak magnitude is bounded by a finite value of y_p^+. Note that (5.9*a*,*b*) also indicates that a 10 % uncertainty of y_p^+ results in a 20 % uncertainty of the magnitude. Note also that $y_p^+ \approx 14$ at $Re = 300$ from a DNS channel (Iwamoto *et al.* 2002), almost the same as $y_p^+ \approx 15$ at $Re = 9 \times 10^5$ from the atmospheric surface layer observation by Metzger & Klewicki (2001), so the Re-variation of y_p^+ is quite weak – if it exists at all. It should be mentioned, however, that the atmospheric surface layer data in Metzger *et al.* (2001) leave open the possibility that y_p^+ may extend beyond 23.

6. Conclusion

The main point of this paper is that the asymptotic value of 1/4 (scaled by u_τ^4/ν) for the maximum turbulent production provides a constraint on the dissipation rate and turbulent diffusion at the wall. The new defect law, $1/4 - \epsilon_w^+ \propto Re^{-1/4}$, indicates that the dissipation rate in the wall region, caused by the small eddies in the viscous range, is influenced by the outer layer directly. This, in turn, leads to a similar defect power-law for the streamwise turbulence intensity peak, i.e. $\overline{u'u'}_\infty^{+} - \overline{u'u'}_p^{+} \propto Re^{-1/4}$, showing a finite turbulent intensity peak near the wall as $Re \to \infty$. We believe that this is a powerful statement, whose qualitative physics is that the smallest scales of the outer layer form the largest scales of the wall layer.

Compared to the logarithmic growth, the present scaling proposals present a similarly good, if not better, description of data for the Re domain currently covered for channel, pipe and TBL flows. At the minimum, it presents an alternative formulation which successfully agrees with the data. Though close to each other at the current Re domain, the most important difference occurs as $Re \to \infty$. While the logarithmic scaling indicates a divergent near-wall peak, the present results predict a finite limit and lend support to the classical wall-scaling for turbulence intensity at asymptotically high Reynolds numbers.

Acknowledgements. We are grateful to all the authors cited in figure 1 (particularly J. Klewicki) for making their data available, to I. Marusic for useful correspondence and to the anonymous referees whose comments improved the paper. X.C. appreciates beneficial discussions with J.C. Vassilicos and J.P. Laval and the funding support by the grants KG16045601 (BUAA) and KZ73030006 (NSFC).

Declaration of interests. The authors report no conflict of interest.

Author ORCIDs.
Xi Chen http://orcid.org/0000-0002-4702-8735.

References

Ahn, J.S., Lee, J.H., Lee, J., Kang, J.-H & Sung, H.J. 2015 Direct numerical simulation of a 30R long turbulent pipe flow at $Re_\tau = 3008$. *Phys. Fluids* **27**, 065110.

Cantwell, B.J. 2019 A universal velocity profile for smooth wall pipe flow. *J. Fluid Mech.* **878**, 834–874.

Chen, X., Hussain, F. & She, Z.S. 2018 Quantifying wall turbulence via a symmetry approach. Part II. Reynolds stresses. *J. Fluid Mech.* **850**, 401–438.

Chen, X., Hussain, F. & She, Z.S. 2019 Non-universal scaling transition of momentum cascade in wall turbulence. *J. Fluid Mech.* **871**, R2.

DeGraaff, D.B. & Eaton, J.K. 2000 Reynolds-number scaling of the flat plate turbulent boundary layer. *J. Fluid Mech.* **422**, 319–346.

Hoyas, S. & Jimenez, J. 2006 Scaling of the velocity fluctuations in turbulent channels up to $Re_\tau = 2003$. *Phys. Fluids* **18**, 011702.

Hultmark, M., Vallikivi, M., Bailey, S.C.C. & Smits, A.J. 2012 Turbulent pipe flow at extreme Reynolds numbers. *Phys. Rev. Lett.* **108**, 094501.

Iwamoto, K., Suzuki, Y. & Kasagi, N. 2002 Database of fully developed channel flow. *Tech. Rep.* ILR-0201. Available at: http://www.thtlab.t.utokyo.ac.jp.

Lee, M. & Moser, R.D. 2015 Direct numerical simulation of turbulent channel flow up to $Re_\tau = 5200$. *J. Fluid Mech.* **774**, 395–415.

Marusic, I., Baars, W.J. & Hutchins, N. 2017 Scaling of the streamwise turbulence intensity in the context of inner-outer interactions in wall turbulence. *Phys. Rev. Fluids* **2**, 100502.

Marusic, I., Chauhan, K.A., Kulandaivelu, V. & Hutchins, N. 2015 Evolution of zero-pressure-gradient boundary layers from different tripping conditions. *J. Fluid Mech.* **783**, 379–411.

Marusic, I., McKeon, B.J., Monkewitz, P.A., Nagib, H.M., Smits, A.J. & Sreenivasan, K.R. 2010 Wall-bounded turbulent flows at high Reynolds numbers: recent advances and key issues. *Phys. Fluids* **22**, 065103.

Metzger, M.M. & Klewicki, J. 2001 A comparative study of near-wall turbulence in high and low Reynolds number boundary layers. *Phys. Fluids* **13**, 692–701.

Metzger, M.M., Klewicki, J.C., Bradshaw, K.L. & Sadr, R. 2001 Scaling the near-wall axial turbulent stress in the zero pressure gradient boundary layer. *Phys. Fluids* **13**, 1819–1821.

Monkewitz, P.A. & Nagib, H.M. 2015 Large-Reynolds-number asymptotics of the streamwise normal stress in zero-pressure-gradient turbulent boundary layers. *J. Fluid Mech.* **783**, 474–503.

Monkewitz, P.A., Chauhan, K.A. & Nagib, H.M. 2007 Self-consistent high-Reynolds-number asymptotics for zero-pressure-gradient turbulent boundary layers. *Phys. Fluids* **19**, 115101.

Nagib, H.M., Chauhan, K.A. & Monkewitz, P.A. 2007 Approach to an asymptotic state for zero pressure gradient turbulent boundary layers. *Phil. Trans. R. Soc. Lond.* A **365**, 755–770.

Örlü, R. 2009 Experimental studies in jet flows and zero pressure-gradient turbulent boundary layers. PhD thesis, KTH Royal Institute of Technology.

Örlü, R. & Alfredsson, P.H. 2013 Comment on the scaling of the near-wall streamwise variance peak in turbulent pipe flows. *Exp. Fluids* **54**, 1431–1435.

Rao, K.N., Narasimha, R. & Narayanan, M.A. 1971 The 'bursting' phenomenon in a turbulent boundary layer. *J. Fluid Mech.* **48**, 339–352.

Samie, M., Marusic, I., Hutchins, N., Fu, M.K., Fan, Y., Hultmark, M. & Smits, A.J. 2018 Fully resolved measurements of turbulent boundary layer flows up to $Re_\tau = 20\,000$. *J. Fluid Mech.* **851**, 391–415.

Schlatter, P., Örlü, R., Li, Q., Brethouwer, G., Fransson, J.H.M., Johansson, A.V., Alfredsson, P.H. & Henningson, D.S. 2009 Turbulent boundary layers up to $Re_\theta = 2500$ studied through simulation and experiment. *Phys. Fluids* **21**, 051702.

She, Z.S., Chen, X. & Hussain, F. 2017 Quantifying wall turbulence via a symmetry approach: a Lie group theory. *J. Fluid Mech.* **827**, 322–356.

Sillero, J.A., Jimenez, J. & Moser, R. 2013 One-point statistics for turbulent wall-bounded flows at Reynolds numbers up to $\delta^+ = 2000$. *Phys. Fluids* **25**, 105102.

Smits, A.J. 2019 Experiments in high Reynolds number flows. *Bull. Am. Phys. Soc.* **64**, 13.

Smits, A.J., McKeon, B.J. & Marusic, I. 2011 High-Reynolds number wall turbulence. *Annu. Rev. Fluid Mech.* **43**, 353–375.

Spalart, P.R. 1988 Direct simulation of a turbulent boundary layer up to $Re_\theta = 1410$. *J. Fluid Mech.* **187**, 61–98.

SREENIVASAN, K.R. 1989 The turbulent boundary layer. In *Frontiers in Experimental Fluid Mechanics* (ed. M. Gad-el-Hak), pp. 159–209. Springer.

TARDU, S. 2017 Near wall dissipation revisited. *Intl J. Heat Fluid Flow* **67**, 104–115.

VALLIKIVI, M., GANAPATHISUBRAMANI, B. & SMITS, A.J. 2015 Spectral scaling in boundary layers and pipes at very high Reynolds numbers. *J. Fluid Mech.* **771**, 303–326.

VINCENTI, P., KLEWICKI, J., MORRILL-WINTER, C., WHITE, C.M. & WOSNIK, M. 2013 Streamwise velocity statistics in turbulent boundary layers that spatially develop to high Reynolds number. *Exp. Fluids* **54**, 1629.

WILCOX, D.C. 2006 *Turbulence Modeling for CFD*. DCW Industries La Canada.

WILLERT, C., SORIA, J., STANISLAS, M., KLINNER, J., AMILI, O., EISFELDER, M., CUVIER, C., BELLANI, G., FIORINI, T. & TALAMELLI, A. 2017 Near-wall statistics of a turbulent pipe flow at shear Reynolds numbers up to 40 000. *J. Fluid Mech.* **826**, R5.

WU, X.H. & MOIN, P. 2008 Direct numerical simulation on the mean velocity characteristics in turbulent pipe flow. *J. Fluid Mech.* **608**, 5–41.

YAMAMOTO, Y. & TSUJI, Y. 2018 Numerical evidence of logarithmic regions in channel flow at $Re_\tau = 8000$. *Phys. Rev. Fluids* **3**, 012602(R).